

Film thickness calculation in elasto-hydrodynamic lubricated line and elliptical contacts: the Dowson, Higginson, Hamrock contribution

A A Lubrecht^{1*}, C H Venner², and F Colin^{1,3}

¹Laboratoire de Mécanique des Contacts, Université de Lyon, INSA-Lyon, LaMCoS, CNRS UMR 5259, Villeurbanne, France

²University of Twente, The Netherlands

³Université de Lyon, Université Claude Bernard, Villeurbanne, France

The manuscript was received on 13 August 2008 and was accepted after revision for publication on 10 November 2008.

DOI: 10.1243/13506501JET508

Abstract: This article traces the contribution of the Dowson and Higginson work to numerical line contact elasto-hydrodynamic lubricated film thickness prediction and the Hamrock and Dowson contribution to the film thickness prediction in elliptical contacts. Considering the line contact work, this article shows that both the numerical pressure and film thickness results and the curve-fitted film thickness predictions are very accurate, even by today's standards. Concerning the elliptical results, the authors show that the original predictions remain surprisingly accurate but that the issue of the minimum to central film thickness ratio H_m/H_c is not yet completely settled.

The article then continues to discuss some limitations of the current models that require additional work, mainly in the area of realistic non-Newtonian lubricant rheology for film thickness predictions and pressure spike analysis.

Keywords: elasto-hydrodynamic lubricant, film thickness, line contact, elliptical contact, numerical solution

1 INTRODUCTION

The introduction of the electronic computer has revolutionized the field of science and technology. In the area of elasto-hydrodynamic lubricated (EHL) film thickness predictions, only few 'analytical' solutions exist. The pioneering numerical work of Dowson and Higginson on the EHL line contact and that of Hamrock and Dowson on the elliptical EHL contact have created an important new field in Tribology: numerical elasto-hydrodynamic lubrication (EHL)! As a result of their work, the film thickness in an EHL contact can be predicted with accuracy from the contact geometry and the operating conditions. Using three dimensionless parameters W , U , and G , they simplified the film thickness representation. The minimum and central

film thickness predictions have been confirmed by various experimental techniques, whereas the qualitative film thickness shape has been experimentally confirmed by optical interferometry. The work has started to analyse the behaviour of the minimum film thickness (and its position in elliptical contacts). Furthermore, the work allowed a qualitative understanding of the pressure spike. Finally, Dowson and Higginson introduced a relation for the lubricant compressibility that is still used to date.

2 LINE CONTACT

The publications [1–3] showed for the first time full numerical film thickness and pressure distributions and a curve fitted minimum film prediction $H^*(W, U, G)$. The incompressible pressure distributions published in reference [1] show very high spikes. When using very fine grids [4], it can be shown that all (incompressible) spikes are even higher than depicted in reference [1]. As even lubricants show some degree

*Corresponding author: Laboratoire de Mécanique des Contacts, INSA-Lyon, Bat J. d'Alembert, 20 Avenue Albert Einstein, Villeurbanne, 69621, France.
email: Ton.Lubrecht@insa-lyon.fr

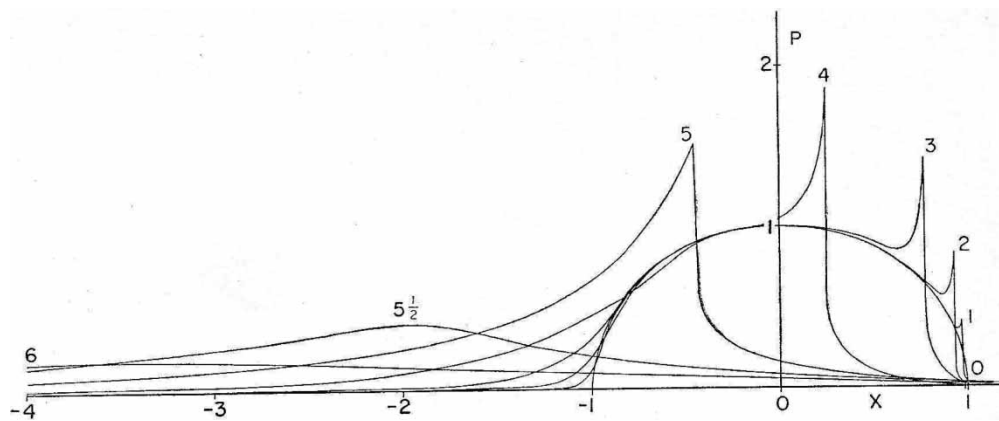


Fig. 1 EHL line contact pressure distributions from reference [2]; vertical scale has been non-dimensionalized with respect to the Hertzian pressure p_h

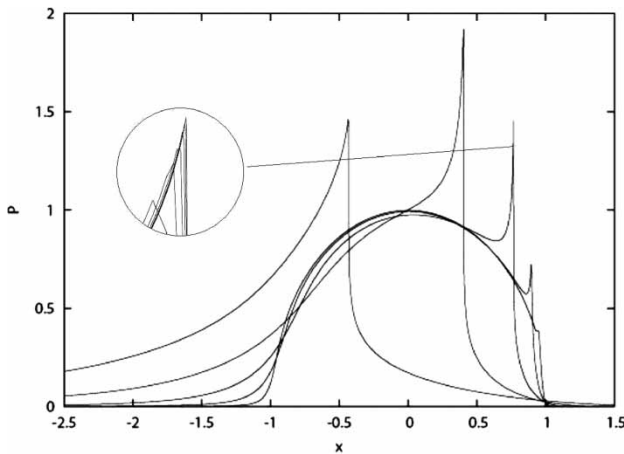


Fig. 2 Grid converged EHL line contact pressure distributions

of compressibility in the GigaPascal pressure range, this discussion is rather academic. Including the compressibility in the numerical calculations results in a significant reduction of the pressure peak height. The comparison between the compressible results from reference [2] (Fig. 1) and more recent results with very fine grids (Fig. 2) shows identical pressure distributions and spike heights, except for some minor details.

The zoom in Fig. 2 shows the convergence of the pressure spike for $U = 10^{-11}$ (horizontal zoom $\times 100$, vertical zoom $\times 10$). The film thickness profiles have not been reported as the differences are not visible on a graph. The accuracy of the nearly 50-year-old numerical solutions is amazing. Even more astonishing is the quality of the film thickness prediction given by the curve fit:

$$H^* = 1.6 G^{0.6} U^{0.7} W^{-0.13}$$

where G , U and W are the dimensionless line contact parameters.

Table 1 Line contact: predicted minimum film thickness versus calculated minimum film thickness as a function of U for a line contact ($W = 3 \times 10^{-5}$, $G = 5000$)

U	H^*	H_{calc}
10^{-9}	5.15×10^{-4}	4.99×10^{-4}
10^{-10}	9.85×10^{-5}	9.81×10^{-5}
10^{-11}	2.05×10^{-5}	2.03×10^{-5}
10^{-12}	4.09×10^{-6}	4.05×10^{-6}
10^{-13}	8.13×10^{-7}	8.05×10^{-7}

Table 1 shows that over a wide range of operating conditions the predicted film thickness is to within 1 per cent of the calculated one. (Care has been taken to obtain grid convergence and avoid numerical starvation.)

From Table 1, it can be concluded that the quality of the EHL line contact results obtained by Dowson and Higginson 50 years ago remains astonishing. As a consequence, their film thickness prediction is still used by designers and engineers all over the world. Moreover, researchers all over the world use the same equation as a reference for their numerical EHL development.

The line contact elastohydrodynamical problem has only a few remaining secrets. The most important issue is the height of the pressure spike using a realistic rheological fluid behaviour (and the related contact fatigue issue). A second major issue is the friction under low-slip sliding conditions, once again using a realistic rheological behaviour. Another more numerical issue remains as well: the solution for high αp_h values. In this case, a dramatic viscosity variation occurs in the entrance region and in the pressure spike region, causing serious convergence problems.

3 CIRCULAR AND ELLIPTICAL CONTACT

Due to computing power limitations, the first circular and elliptical pressure and film thickness solutions

required almost two more decades [5, 6]. Because of its two-dimensional nature, the solution of the elliptical contact problem inherently requires a larger computational effort than the line contact solution. However, the elliptical problem has two additional issues: the ellipticity itself adds another dimension to the parameter space and the ratio minimum to central film thickness is not a constant as in the line contact case. A related problem is the minimum film thickness position: it is either found in the side lobe region or on the centre line $Y = 0$. The H_m/H_c ratio is a function of the operating conditions including the ellipticity. Hence, two predictions are required

$$H_m = 3.63 G^{0.49} U^{0.68} W^{-0.073} (1 - e^{-0.68k})$$

$$H_c = 2.69 G^{0.53} U^{0.67} W^{-0.067} (1 - 0.61e^{-0.73k})$$

Figure 3 shows the evolution of the film thickness distribution as a function of the ellipticity, scaled onto a circle (using $X = x/a$ and $Y = y/b$). It can be observed that the minimum film thickness occurs in the side lobes only for close-to-circular contacts. For

wide elliptical contacts, the minimum occurs on the centreline $Y = 0$.

Tables 2 and 3 show the evolution of the central and minimum film thickness as a function of the ellipticity, maintaining Hertzian pressure and mean speed. The two tables use different values of the αp_h value. Throughout the range of EHL operating conditions, the minimum and central film thickness maintain an error smaller than a few percent. For larger R_y/R_x values ($R_y/R_x > 10$), the elliptical problem tends towards the equivalent line contact result for both the central and minimum film thickness. The influence of the αp_h parameter on this behaviour seems limited. The Hamrock–Dowson predictions continue to evolve.

Figure 4 shows the film thickness distribution in the Y -direction (between $(0, Y)$ and $(0, 0)$) and in the X -direction (between $(0, 0)$ and $(X, 0)$) (line in Fig. 3(a)). The ellipticity was varied in the calculation, while maintaining the maximum Hertzian pressure p_h constant as well as the mean velocity u_m . From this figure, it can be concluded that for these operating conditions and for $R_y/R_x > 10$, the central and minimum film thickness tend to an asymptotic value: the

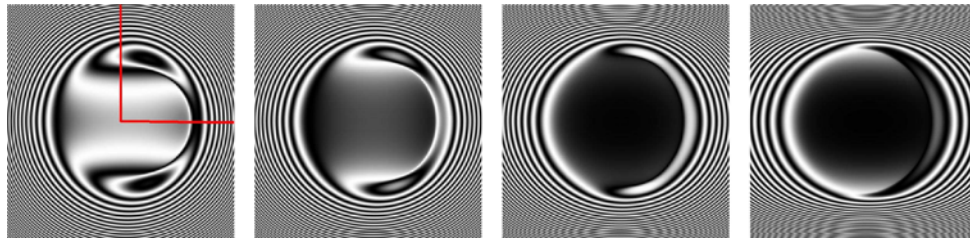


Fig. 3 Elliptical contact film thickness distribution for $R_y/R_x = 1.0, 2.0, 5.0, 50.0$ (see Table 2 for the operating conditions)

Table 2 Predicted central H_c and minimum film thickness H_m versus calculated values as a function of ellipticity, for $U = 1.68 \times 10^{-12}$ and $G = 4520$

R_y/R_x	W	H_c	$H_{c\text{-calc}}$	H_m	$H_{m\text{-calc}}$
1.0	1.11×10^{-7}	6.28×10^{-6}	6.30×10^{-6}	3.59×10^{-6}	3.66×10^{-6}
2.0	2.13×10^{-7}	6.84×10^{-6}	6.53×10^{-6}	4.51×10^{-6}	4.33×10^{-6}
5.0	4.48×10^{-7}	7.43×10^{-6}	6.61×10^{-6}	5.53×10^{-6}	5.19×10^{-6}
10.0	7.45×10^{-7}	7.58×10^{-6}	6.43×10^{-6}	5.91×10^{-6}	5.39×10^{-6}
20.0	1.19×10^{-6}	7.49×10^{-6}	6.42×10^{-6}	5.94×10^{-6}	5.38×10^{-6}
50.0	2.13×10^{-6}	7.23×10^{-6}	6.41×10^{-6}	5.74×10^{-6}	5.37×10^{-6}
100.0	3.25×10^{-6}	7.03×10^{-6}	6.40×10^{-6}	5.57×10^{-6}	5.37×10^{-6}

Table 3 Predicted central H_c and minimum film thickness H_m versus calculated values as a function of ellipticity, for $U = 2.70 \times 10^{-11}$ and $G = 4520$

R_y/R_x	W	H_c	$H_{c\text{-calc}}$	H_m	$H_{m\text{-calc}}$
1.0	8.86×10^{-7}	3.50×10^{-5}	3.62×10^{-5}	2.03×10^{-5}	2.26×10^{-5}
2.0	1.70×10^{-6}	3.81×10^{-5}	3.78×10^{-5}	2.56×10^{-5}	2.66×10^{-5}
5.0	3.58×10^{-6}	4.14×10^{-5}	3.84×10^{-5}	3.13×10^{-5}	3.15×10^{-5}
10.0	5.96×10^{-6}	4.22×10^{-5}	3.82×10^{-5}	3.35×10^{-5}	3.32×10^{-5}
20.0	9.54×10^{-6}	4.17×10^{-5}	3.82×10^{-5}	3.36×10^{-5}	3.31×10^{-5}
50.0	1.71×10^{-5}	4.03×10^{-5}	3.80×10^{-5}	3.25×10^{-5}	3.29×10^{-5}
100.0	2.60×10^{-5}	3.92×10^{-5}	3.79×10^{-5}	3.15×10^{-5}	3.27×10^{-5}

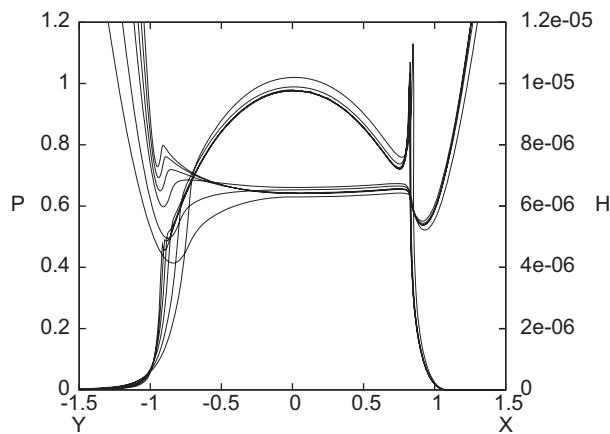


Fig. 4 Pressure and film thickness as a function of Y and X for $R_y/R_x = 1.0, 2.0, 5.0, 10.0, 20.0, 50.0$, $H(Y)$ bottom to top

equivalent line contact. The elliptical integrals were approximated according to reference [7]. By comparing the two local minima, it can be concluded that the global minimum film thickness occurs in the side lobes for more or less circular contacts. For wide elliptical contacts, the global minimum is situated on the $Y = 0$ centreline of the contact. For these very wide contacts, the local side lobe minimum can exceed the central film thickness. The minimum film thickness in the side lobes increases with the ellipticity because the pressure gradient dP/dY decreases with ellipticity. The same effect accounts for the diminishing pressure spike when moving away from the centreline. The fact that the local minimum can exceed the central value is caused by the compressibility effect.

Hamrock and Dowson were the first to attempt to predict the minimum and central film thickness values. Chittenden *et al.* [8], Hooke [9], and Nijenbanning *et al.* [10] produced different predictions, but a single prediction for wide and slender elliptical contacts and for the central and the two minima has not yet been published.

Hamrock and Dowson [11] also addressed the starved lubrication problem: that is the film thickness prediction when the amount of lubricant present in the inlet is limited. As a consequence, the central and minimum film thickness are smaller than the fully flooded values and both pressure and film thickness distribution tend to the Hertzian asymptote. In more recent work, the meniscus position, which they used as a starvation parameter, has been replaced by the oil film thickness present on the surfaces in the contact inlet.

Compared with the line contact elastohydrodynamic problem, the point contact has more remaining secrets: first and foremost, a simple and robust prediction of the minimum and central film thickness for wide and slender elliptical contacts. A second important issue is the height of the pressure spike using a

realistic rheological fluid behaviour (and the related contact fatigue issue). The third issue is the friction under low-slip sliding conditions, once again using a realistic rheological behaviour. Finally, a predictive tool for the rolling friction $\iint p(dh/dx) dx dy$ and the convergence at higher αp_h values require attention.

4 CONCLUSION

The pioneering work of Dowson and Higginson on the EHL line contact problem and that of Hamrock and Dowson on the EHL elliptical contact problem has proven to be lasting contributions to the Tribological literature and to design rules for machine elements. Their minimum film thickness line contact H^* prediction has remained the standard equation in the EHL regime. Furthermore, their H_c elliptical contact equation is the standard equation for EHL elliptical contacts.

Building on their results other solvers have emerged, currently allowing researchers to study the EHL contact in more and more detail. Among these extensions feature: solvers for transient conditions, lubrication of rough and textured surfaces, EHL using more complex rheological lubricant models, lubrication with important thermal effects, starved lubrication, etc., and of course combinations of all these phenomena.

ACKNOWLEDGEMENTS

The first author is indebted to A. Nijkamp for facilitating the completion of this paper.

REFERENCES

- 1 Dowson, D. and Higginson, G. R. A numerical solution to the elastohydrodynamic problem. *J. Mech. Eng. Sci.*, 1959, **1**, 6.
- 2 Dowson, D., Higginson, G. R., and Whitaker, A. V. Elastohydrodynamic lubrication: a survey of isothermal solutions. *J. Mech. Eng. Sci.*, 1961, **4**, 121–126.
- 3 Dowson, D. and Higginson, G. R. *Elastohydrodynamic lubrication, the fundamentals of roller and gear lubrication*, 1966 (Pergamon Press, Oxford, Great Britain).
- 4 Venner C. H. and Lubrecht A. A. *Multilevel methods in lubrication*, vol. 37, 2000, p. 379 (Elsevier, Amsterdam).
- 5 Hamrock, B. J. and Dowson, D. Isothermal elastohydrodynamic lubrication of point contacts, part I, theoretical formulation. *ASME J. Lubr. Tech.*, 1976, **98**, 223–229.
- 6 Hamrock, B. J. and Dowson, D. Isothermal elastohydrodynamic lubrication of point contacts, part III, fully flooded results. *ASME J. Lubr. Tech.*, 1977, **99**, 264–276.
- 7 Moes, H. Lubrication and beyond. In *Lecture notes*, 2000, p. 386 (Twente University), available from the University of Twente server <http://www.tr.ctw.utwente.nl/Organisation/Links/index.html>.

- 8 Chittenden, R. J., Dowson, D., Dunn, J. F., and Taylor, C. M.** A theoretical analysis of the isothermal elastohydrodynamic lubrication of concentrated contacts I: direction of lubricant entrainment coincident with the major axis of the contact ellipse. *Proc. R. Soc. London*, 1985, **A397**, 345–369.
- 9 Hooke, C. J.** An interpolation procedure for the minimum film thickness in point contacts. *Proc. IMechE, Part C: J. Mechanical Engineering Science*, 1990, **204**, 199–206.
- 10 Nijenbanning, G., Venner, C. H., and Moes, H.** Film thickness in elastohydrodynamically lubricated elliptic contacts. *Wear*, 1994, **176**, 217–229.
- 11 Hamrock, B. J. and Dowson, D.** Isothermal elastohydrodynamic lubrication of point contacts, part IV, starvation results. *ASME J. Lubr. Tech.*, 1977, **99**, 15–23.

APPENDIX

Notation

- a contact half width in rolling direction
 b contact half width perpendicular to rolling direction
 E' reduced elastic modulus
 G dimensionless materials parameter
 $G = \alpha E'$

- h film thickness
 H dimensionless film thickness
 $(H = h/R_x)$
 H^*, H_m dimensionless minimum film thickness (one- and two-dimensional)
 H_c dimensionless central film thickness
 p pressure (Pa)
 p_h maximum Hertzian pressure (Pa)
 P dimensionless pressure ($P = p/p_h$)
 R_x reduced radius of curvature in x -direction
 R_y reduced radius of curvature in y -direction
 u_m mean velocity in x -direction
 $(u_m = (u_1 + u_2)/2)$
 U dimensionless speed parameter
 $(U = (\eta_0 u_m)/(E'R_x))$
 w load (per unit length (one-dimensional))
 W dimensionless load parameter
 $W = w/(E'R_x)$, $W = w/(E'R_x^2)$ (one- and two-dimensional, respectively)
 X, Y dimensionless coordinates ($X = x/a$, $Y = y/b$)
 α viscosity pressure coefficient (Pa^{-1})
 η_0 viscosity at ambient pressure (Pa s)
 ρ_0 density at ambient pressure (kg/m^3)